Phase-separation kinetics in concentrated solutions of linear diblock copolymers of polystyrene and polyisoprene from time-resolved small-angle neutron scattering

James G. Connell* and Randal W. Richards*†
Department of Pure and Applied Chemistry, University of Strathclyde, Glasgow G1 1XL, UK

and Adrian R. Rennie
Institut Laue-Langevin, 38042 Grenoble, France
(Received 27 March 1990; revised 5 June 1990; accepted 11 June 1990)

Concentrated solutions of block copolymers of polystyrene and polyisoprene have been quenched from a high temperature to a lower temperature. The changes in scattering intensity following such a quench were studied using time-resolved small-angle neutron scattering. From these data the rate constant for the relaxation process, $R(Q)$, was obtained as a function of scattering vector Q. For high concentrations, a maximum in $R(Q)$ as a function of Q^2 was observed as predicted by a time-dependent Ginzburg–Landau model. Values of the Onsager coefficient L_O, extracted from these data were several orders of magnitude smaller than those for homopolymer blends.

(Keywords: block copolymers; phase-separation kinetics; time-resolved scattering)

INTRODUCTION

The possible advantages obtainable by molecularly mixing two or more chemically distinct monomers to form a homogeneous blend have provoked much interest in the theory and experimentation on these systems. Considerable effort has been expended on thermodynamic descriptions of polymer blends[1–3], and this has led to experimental studies of the phase diagrams and the factors controlling miscibility[4–6]. A notable feature of this work has been the interest in the *kinetics* of phase separation of homopolymer blends. Such studies provide an insight into the mechanism of phase separation and are a link between thermodynamics and dynamics of polymer motion. Much interpretation of phase-separation kinetics has resulted from a straightforward application of the theory[7] of spinodal decomposition originally applied to metal alloys. Significant extensions specific to polymer systems that bring in reptation theory have been made by de Gennes[8], Pincus[9] and Binder[10].

Block copolymers differ from homopolymer blends due to the molecular connectivity between the chemically distinct blocks that make up the molecule. This connectivity considerably alters the thermodynamics and kinetics of phase separation due to the reduction in entropy relative to the equivalent homopolymer blend. The most obvious effect of this connectivity is in the formation of microphase-separated domains[11] when the thermodynamic driving force for demixing exceeds a critical value. Additionally, the connectivity of block copolymers means that the scattering law in the homogeneous, disordered (usually high-temperature) phase is radically different from that of a homopolymer blend[12–14]. Hence, rather than a continuous decrease in scattered intensity (X-rays, neutrons) with increase in scattering vector Q, as observed for homopolymers, a maximum at a finite Q value is seen for block copolymers. This was termed a 'correlation hole effect' by de Gennes, and was discussed in detail by Leibler using the random-phase approximation (RPA)[12]. Subsequently the problem has been analysed in more detail by Fredrickson and Helfand[13] and others[14]. Furthermore, block copolymer types other than linear diblocks and mixtures of copolymers with homopolymers have also been discussed and the scattering laws in the homogeneous one-phase region reported[15].

Experimental studies utilizing the RPA have been limited, the earliest reported results being those of Hashimoto[16] on a linear diblock. In an earlier paper[17] we discussed very concentrated solutions of block copolymers in the light of RPA theory. Star block copolymers have also been examined both in the bulk state and dissolved in a non-selective solvent[18,19].

Studies of the kinetics of phase transitions in block copolymers are sparse. To our knowledge only one detailed report of the order–disorder transition has been published[20]. However, it is clear that other data exist but have yet to be thoroughly discussed[21]. This sparsity of data may be in part due to the spatial extent of the concentration fluctuations driving the phase-separation process. In homopolymer blends these rapidly grow to dimensions observable by small-angle light scattering,

* Present address: Interdisciplinary Research Centre for Polymer Science and Technology, Department of Chemistry, University of Durham, South Road, Durham DH1 3LE, UK
† To whom correspondence should be addressed

0032-3861/91/112033-10

whereas the connectivity in block copolymers restricts these fluctuations to colloidal dimensions (~200 Å). Consequently, observation calls for small-angle X-ray or neutron scattering (SAXS or SANS). In this paper we present results obtained by time-resolved SANS from very concentrated solutions of a styrene–isoprene linear diblock copolymer on either sudden cooling from a high-temperature homogeneous disordered phase to a lower temperature in the disordered phase or a deep quench from the high-temperature phase into the ordered phase. We demonstrate the use of isotopic labelling to improve the signal-to-noise ratio in SANS and outline the general technique in time-resolved small-angle scattering experiments. The data are analysed by a generalized time-dependent Ginzburg–Landau model of microphase-separation kinetics proposed by Hashimoto[21] for block copolymer systems.

THEORY

The phase state of a block copolymer may be described by a local order parameter specified for one component $\psi(\boldsymbol{r})$. This order parameter is the difference between the average monomer unit density in the homogeneous phase and the local density of the same monomer units. In the one-phase disordered region, $\psi(\boldsymbol{r}) = 0$. As the system undergoes phase separation, $\psi(\boldsymbol{r})$ fluctuates markedly from 0, and the range of these fluctuations can be described by a density–density correlation function:

$$S(\boldsymbol{r} - \boldsymbol{r}') \propto \langle \psi(\boldsymbol{r})\psi(\boldsymbol{r}') \rangle \tag{1}$$

On the basis of being in qualitative agreement with the features observed experimentally, Hashimoto[21] proposed that the time variation of the order parameter in a block copolymer system quenched to a lower temperature from an initially homogeneous state is given by a time-dependent Ginzburg–Landau theory[22]. The equation describing this is a diffusion equation of the Langevin type, which in reciprocal space is:

$$\mathrm{d}\psi(Q, t)/\mathrm{d}t = L_{\mathrm{O}} Q^2 \psi(Q, t)[-S(Q)^{-1}] \tag{2}$$

where $\psi(Q, t)$ is the local order parameter at time t after the quench, L_{O} is an Onsager coefficient connecting the diffusive flux of copolymer molecules to the local chemical potential, $S(Q)$ is the Fourier transform of the density–density correlation function (i.e. the scattering law) for the homogeneous state, and Q is the scattering vector ($(4\pi/\lambda) \sin\theta$ for radiation of wavelength λ and scattering angle 2θ). Therefore:

$$\psi(Q, t) = \psi(Q, 0) \exp[R(Q)t] \tag{3}$$

$$R(Q) = L_{\mathrm{O}} Q^2 [-S(Q)^{-1}] \tag{4}$$

Since

$$I(Q) = \langle |\psi(Q)|^2 \rangle \tag{5}$$

then

$$I(Q, t) = I(Q, 0) \exp[2R(Q)t] \tag{6}$$

Thus, although the general form of the variation of scattered intensity with time at fixed Q following a quench is given by equation (6), the Q variation at a given time interval is determined by the scattering law, $S(Q)$, in the homogeneous state. As remarked above, the random-phase approximation has been used to obtain theoretical expressions for $S(Q)$. The original derivation of Leibler[12] is most appropriate to the experiments to be discussed here, i.e. the weak segregation limit. Weak segregation implies that the density profile corresponding to the concentration fluctuations varies smoothly from region to region. Leibler's expression for $S(Q)$ is:

$$S(Q) = \{[S'(Q)/W(Q)] - 2\chi\}^{-1} \tag{7}$$

where $S'(Q)$ is the sum of the Fourier transforms of the individual density–density correlation functions in the block copolymer system and $W(Q)$ is their determinant. The factor χ is the Flory–Huggins interaction parameter between the components of the block copolymer. For a diblock AB copolymer with the average composition of A blocks being ϕ_{A}, the final expression for $S(Q)$ is:

$$S(Q) = N/[F(x) - 2\chi N] \tag{8}$$

where N = degree of polymerization of block copolymer and:

$$F(x) = g(1, x)/g(\phi_{\mathrm{A}}, x)g(\phi_{\mathrm{B}}, x) - 0.25[g(1, x) - g(\phi_{\mathrm{A}}, x) - g(\phi_{\mathrm{B}}, x)]^2 \tag{9}$$

Here $g(\phi_i, x)$ is the Debye function for the scattering from a single block copolymer molecule, with volume fraction of the component being ϕ_i:

$$g(\phi_i, x) = (2/x^2)[\phi_i x + \exp(-\phi_i x) - 1] \tag{10}$$

and $x = Q^2 R_{\mathrm{g}}^2$ with R_{g} as the radius of gyration of the whole block copolymer molecule.

The form and dependence of equation (8) on R_{g}, N and χ have been much discussed in other publications[12,15,23]. Essentially $S(Q)$ has a broad maximum at $Q_{\max} \simeq 2/R_{\mathrm{g}}$, the breadth of which is determined by χ. As χ increases (thermodynamically poorer situations) the amplitude of the scattering increases and the peak width narrows. At the spinodal point equation (8) diverges and is no longer a true description of the scattering for $\chi \geqslant \chi_{\mathrm{s}}$ ($T \leqslant T_{\mathrm{s}}$), where χ_{s} is the interaction parameter at the spinodal temperature T_{s}. This divergence and its variation with ϕ_i define the phase boundary for the block copolymer. The nature and controlling factors of this phase boundary relative to that for a homopolymer blend have been extensively discussed elsewhere[15].

Equation (6) is a simplified form since it omits the random thermal fluctuations discussed by Cook[24]. Equation (6) further assumes that the Onsager coefficient is Q-independent, which may be valid for early stages of phase separation and a shallow quench, i.e. to temperatures where $\chi \geqslant \chi_{\mathrm{s}}$. Despite these apparent simplifications, equation (6) is sufficient to analyse the experimental data.

The influences of the polymer–polymer interaction parameter χ and L_{O} on the variation of $R(Q)/Q^2$ are instructive and are shown in *Figures 1a* and *1b*. In point of fact the important parameter determining the position with respect to the phase boundary is the product $N\chi$. For values of $N\chi < N\chi_{\mathrm{s}}$, $R(Q)$ is negative. Now $R(Q)/L_{\mathrm{O}}Q^2$ is the thermodynamic driving force for the growth of the concentration fluctuation with wavevector $Q/2\pi$. Negative values indicate that these fluctuations do not grow but decay, i.e. the system remains stable to concentration fluctuations of this wavevector. For $N\chi > N\chi_{\mathrm{s}}$ a very different situation prevails; there is a region of Q wherein $R(Q)/Q^2$ is positive and the concentration fluctuations will grow, eventually leading to phase separation. However, these growing concentration fluctuations have upper and lower critical boundaries to their

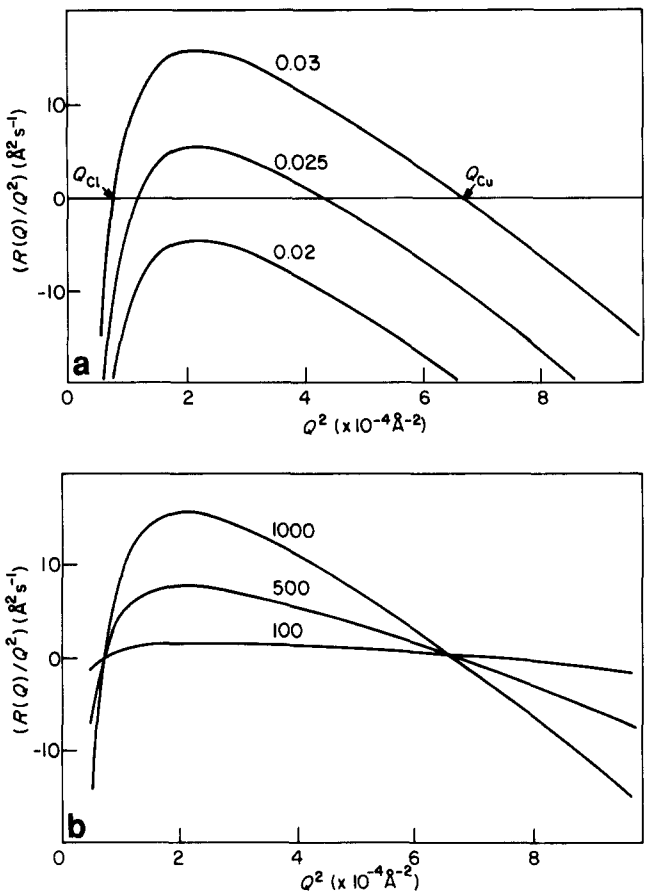

Figure 1 (a) Influence of χ on $R(Q)/Q^2$; χ values marked on each curve, $R_g = 143$ Å, $\phi_{PS} = 0.2$, $N = 1153$, $L = 1000$ Å^2 s^{-1}. (b) Influence of Onsager coefficient L_O on $R(Q)/Q^2$. Values of L_O (Å^2 s^{-1}) marked on each curve; $\chi = 0.03$; all other parameters as in (a)

wavenumbers calculable from the values Q_{Cu} and Q_{Cl} marked on *Figure 1a*. Outside these limits the concentration fluctuations decay and do not contribute to the phase-separation dynamics. It should be made clear that negative values of $R(Q)$, whether arising from a quench *within* the disordered regime or observed at a Q value outside the critical limits for a quench below the spinodal curve, do *not* lead to a reduction in $S(Q)$ in any range of Q. In truth, equation (6) is an oversimplification; if $R(Q)$ is positive then at $t = \infty$ the scattered intensity is infinite; conversely, if $R(Q)$ were negative the scattered intensity would be zero at infinite time following a quench. Equation (6) may be modified[25] to take this into account:

$$I(Q,t) = [I(Q,0) - I(Q,\infty)] \exp[2R(Q)t] + I(Q,\infty) \quad (6a)$$

where $I(Q, \infty)$ is determined by the scattering law $S(Q)$, which prevails at the new equilibrium temperature following a quench. Equation (6a) now exhibits the correct limiting behaviour whether $R(Q)$ is positive or negative. The sign of $R(Q)$ depends on $S(Q)$. Within the homogeneous temperature region, equation (7) is always positive and hence $R(Q)$ is *always* negative. When the system is quenched to a temperature below the micro-phase-separation temperature, equation (7) becomes divergent over the finite range of Q between Q_{Cl} and Q_{Cu}. This results in $R(Q)$ becoming positive; i.e. the concentration fluctuations between these wavelengths grow in amplitude and eventually result in phase separation.

Comparison with linear Cahn–Hilliard theory

As originally published, the Cahn–Hilliard[7] theory is a macroscopic description and has no direct relation to events at a molecular level. Extensions to the theory have been made by de Gennes[8], Pincus[9] and particularly Binder[10] for polymer blends. These authors were particularly concerned with using reptation dynamics in discussing spinodal decomposition. However, we can write the identity:

$$R(Q) = -M(\mathrm{d}^2A/\mathrm{d}c^2)Q^2 - 2MKQ^4 \quad (11)$$

where M = mobility term, A = Helmholtz free energy and K = gradient free-energy term. The Onsager coefficient L_O and M are related by:

$$M = L_O V_{ref}/RT \quad (12)$$

Consequently, taking the analogy further, the effective diffusion coefficient can be calculated from the Q value where the maximum scattering intensity is observed during the demixing process, Q_m, using the relation:

$$D_{eff} = -2R(Q_m)/Q_m^2 \quad (13)$$

Binder[10] provides equations that are identical in form to the Cahn–Hilliard equations but are couched in terms of the diffusion coefficients of the individual components of the homopolymer blend. Moreover, he provides equations for the Onsager coefficient L_O using molecular parameters of the molecules.

EXPERIMENTAL

Polymer preparation

Linear diblock copolymers of deuterostyrene and isoprene were prepared using high-vacuum techniques and n-butyllithium as initiator. Benzene was used as the polymerization solvent and the reaction was terminated by addition of methanol. After isolation and drying under vacuum, the copolymers were analysed by elemental analysis and u.v. spectrometry. Molecular-weight distributions were obtained by size exclusion chromatography and absolute molecular weights obtained from membrane osmometry. *Table 1* reports the composition and molecular weights of the block copolymer used in this study.

Small-angle neutron scattering

All SANS data were collected using the D11 diffractometer at the Institut Laue–Langevin, Grenoble, France. For the purposes of time-resolved scattering following a quench from a high temperature to a lower one, it was necessary to construct a two-stage cell jacket, a schematic diagram of which is shown in *Figure 2*[26]. The block copolymer sample (*vide infra*) was enclosed in a quartz cell placed in a light metal carrier at the end of a rod. The carrier plus sample were initially held in the small upper cell by a solenoid. Circulation of silicone oil from an external thermostat equilibrated the copolymer to a temperature well above the order–disorder temperature.

Table 1 Styrene–isoprene block copolymer characteristics

Weight fraction styrene	$M_w/10^3$	$M_n/10^3$
0.19	85.63	82.14

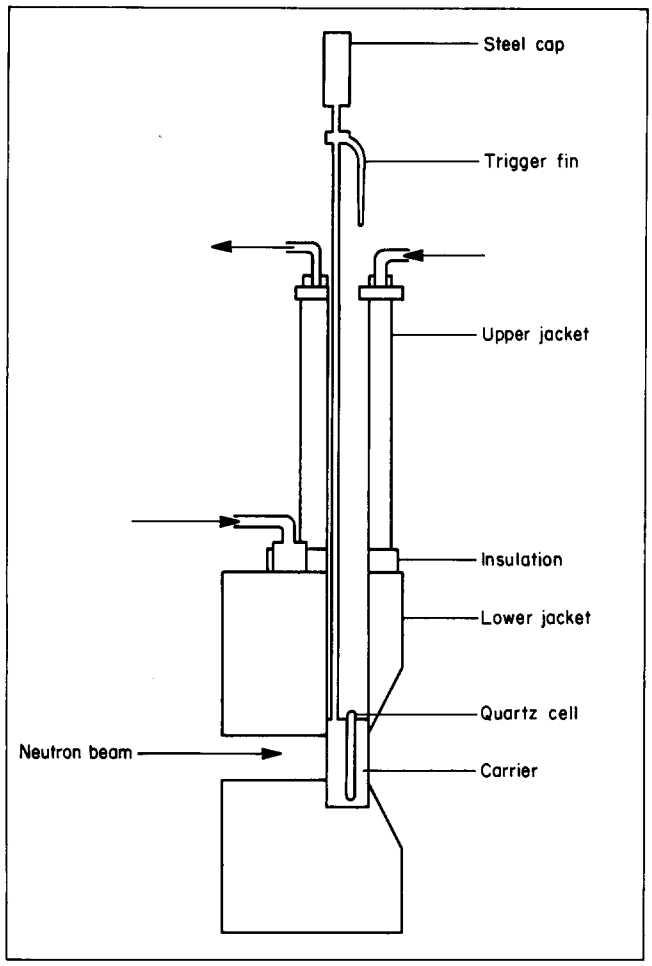

Figure 2 Schematic diagram of heating cell arrangement used in small-angle neutron scattering experiments

After a suitable equilibration time (15–30 min), the current to the solenoid was switched off and the cell plus carrier fell under gravity into the massive lower jacket thermostatted at a lower temperature. As the cell assembly fell an optoelectronic switch was triggered which started the counting electronics of the neutron detector immediately the cell was in position. The electronics could be 'gated' such that scattered intensities were collected for a series of individual time frames after the trigger pulse. On completion of data collection the whole cycle was repeated and the counts from the same time frame added together. Usually, it was necessary to repeat this cycle at least 10 times to obtain an acceptable signal-to-noise ratio. Time frame widths were variable between a minimum of 2 s and a maximum of 32 s, and a maximum of 32 frames were possible, i.e. the shortest time observable was ~2 s, the longest ~17 min. Corrections to the data were made for beam attenuation due to transmission and scattering from the quartz of the cell.

For time-resolved scattering experiments to be successful, it is important to maximize the efficiency of heat transfer to or from the system. With this in mind, our experiments were made on concentrated solutions of the block copolymer in cyclohexane. The presence of solvent molecules aids heat transfer; moreover, the presence of solvent reduces the viscosity, thereby enabling an easier transition to or from the homogeneous phase. Additionally, the presence of solvent *reduces* χ, and thus the transition temperature to the homogeneous phase becomes accessible at a lower temperature. As a counter to these advantages, the reduction in viscosity reduces the time range over which the microphase separation may be observable. *Table 2* gives the scattering length densities of components in the block copolymer solution. The deutero isomer of cyclohexane was incorporated into the solvent mixture at mole fraction of 0.078. This solvent mixture has the same scattering length density as hydrogenous isoprene and therefore the excess scattering over that of the background was not complicated by different contrast factors for the two blocks with the solvent. The concentration range of the solutions studied was from 50% (w/w) to 77% (w/w) block copolymer. Solutions were prepared by placing the desired amount of block copolymer in a 1 mm path length quartz cell fitted with a graded glass seal. To this was added a small quantity of 2,6-di-butyl-4-methylphenol as antioxidant. The correct amount of the C_6H_{12}/C_6D_{12} mixture was added and the cell attached to a vacuum line. After freezing in an acetone/solid carbon dioxide bath, the cells were evacuated and then dry nitrogen introduced. After this procedure, the cells were then flame sealed and stored at 333 K with occasional agitation for a long period before SANS measurements were made on the solutions.

Table 2 Scattering length densities of components of copolymer solutions

Component	ρ (10^{-10} cm^{-2})
d-Styrene	6.30
h-Isoprene	0.27
d-Cyclohexane	6.72
h-Cyclohexane	−0.28

For the block copolymer specimen used, the scattering patterns were radially isotropic around the centre of the detector. These data were radially regrouped using computer programs specific to that purpose; the final form of the data was as a scattering profile of intensity as a function of scattering vector Q.

RESULTS

Thermal response

Before undertaking the time-resolved SANS experiments, it was necessary to determine the thermal response of the apparatus following a quench. For this purpose a cell was filled with silicone oil and a thermocouple inserted into it. This was then placed in the carrier and the whole inserted into the upper cell jacket of *Figure 2*, which was thermostatted at 374 K. When the temperature of the quartz cell and its contents were at equilibrium, the carrier plus cell was allowed to fall into the lower jacket thermostatted at a known lower temperature. The sample cell temperature was recorded at 5 s intervals until it had reached the temperature of the lower jacket. This was performed for six different temperatures of the lower jacket in the range 324 to 368 K. *Figure 3* shows the variation of temperature as a function of time for all of the final temperatures studied. Each curve was describable by the equation:

$$[T(t) - T_f]/(T_i - T_f) = \exp(-t/\tau) \qquad (14)$$

where $T(t)$ is the temperature at time t after a quench from an initial temperature T_i to a final temperature T_f

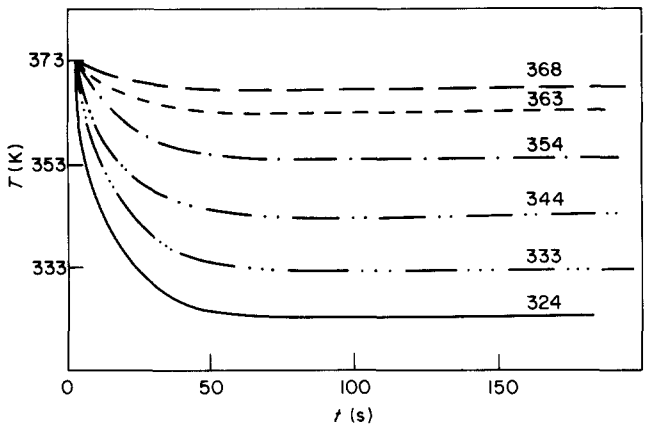

Figure 3 Observed variation in temperature for sudden quenches from 374 K to the temperature marked on each curve

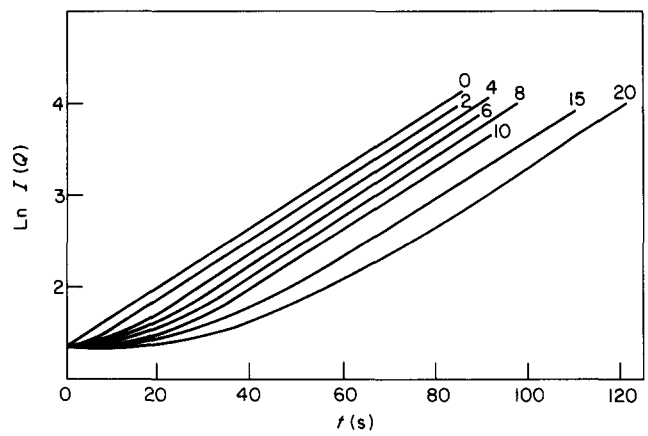

Figure 4 Influence on thermal relaxation time on the increase in intensity for a quench from 374 K to 324 K; $Q = 0.02$ Å^{-1}. Values of τ are marked on each curve

and τ is the relaxation time of the process[27]. Analysing the data in *Figure 3* according to equation (14) gave a mean relaxation time of 14.3 s with a standard deviation of 0.7 s for all quenches. The predicted influence of such a non-ideal temperature drop on the scattered intensity for a quench within the one-phase region was calculated using a multistep temperature jump procedure. For this purpose, the scattering at a time t_j after the quench is related to that for time t_{j-1} by the equation:

$$I(Q, t_j) = I(Q, t_{j-1}) \exp[2Q^2 R(Q, T_{j-1})] \quad (15)$$

where $R(Q, T_{j-1})$ is the relaxation rate constant of the copolymer system at time t_{j-1} where the temperature is T_{j-1} (ref. 27). Evidently, to utilize equation (15), the temperature variation of $R(Q)$ must be known. We have obtained this from data for one of our specimens (*vide infra*). The temperature at a time t_{j-1} is calculated from equation (15) for known values of T_i and T_f and an assumed value of τ. This temperature was then used to evaluate $R(Q, T_{j-1})$ and subsequently to calculate $I(Q, t_j)$; hence the influence of the relaxation time on the scattering as a function of time could be calculated. *Figure 4* shows such curves calculated for a fixed value of Q and for a deep quench. Evidently, at short times the scattered intensity has a non-exponential growth, and the extent of this region grows as the relaxation times increase. However, at sufficiently long times following the quench, the growth in scattered intensity becomes exponential and of the same slope no matter what the value of τ. This simulation suggested that, for our apparatus, the exponential growth in intensity following a quench should be observable ~20 s after the quench. We also investigated the thermal response of the apparatus following a sudden increase in temperature. For the same temperature difference as the quench in *Figure 4*, the relaxation time for a sudden increase in temperature was ~56 s. Such long relaxation times make positive temperature jumps unfeasible as a method of investigating the short-time kinetics of phase transitions in block copolymer systems.

Time-resolved scattering

SANS intensities as a function of time following a quench were recorded for copolymer solutions with copolymer concentrations of 50, 58, 60 and 71% w/v; these are named S50, S58, S60 and S71 respectively. Earlier equilibrium data had provided the microphase-separation temperature (*MST*). *Figure 5* shows typical examples of the change in scattering profile observed for a quench within the disordered region, i.e. $T_f > MST$ and for a quench into the temperature range where a microphase-separated state exists ($T_f < MST$). For the former case, *Figure 5a* shows the expected behaviour: an increase in intensity over all Q values as time increases, and a narrowing of the peak as time increases. In the main these observations are also true for a quench to $T_f < MST$ (*Figure 5b*); however, there is a major difference. Close examination of the scattered intensities at very low Q values (<0.01 Å^{-1}) reveals that the

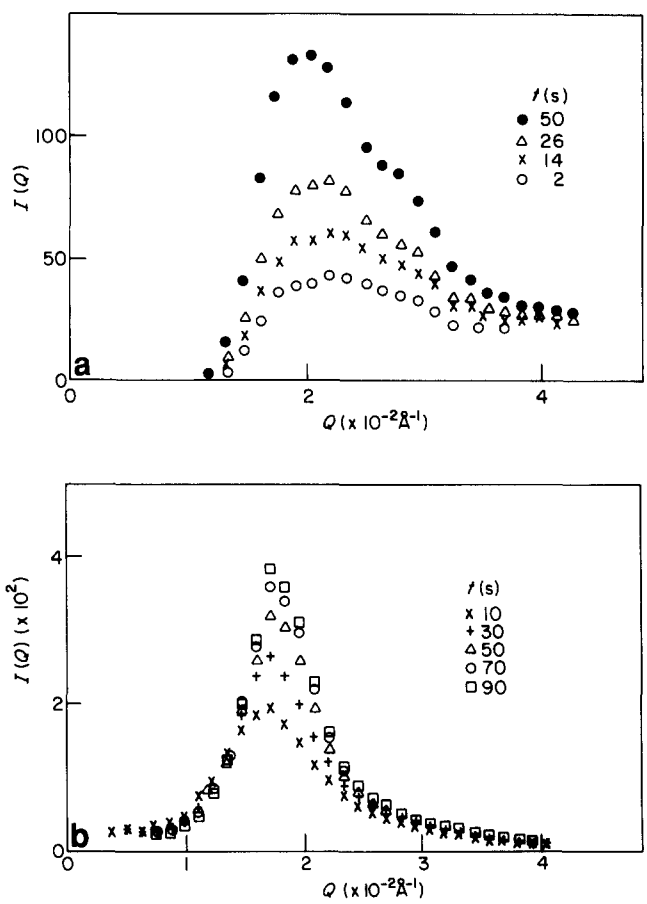

Figure 5 (a) Variation in intensity with time after a quench from 382 K to 337 K for copolymer S58. (b) As in (a) for copolymer S71 quenched from 374 K to 333 K

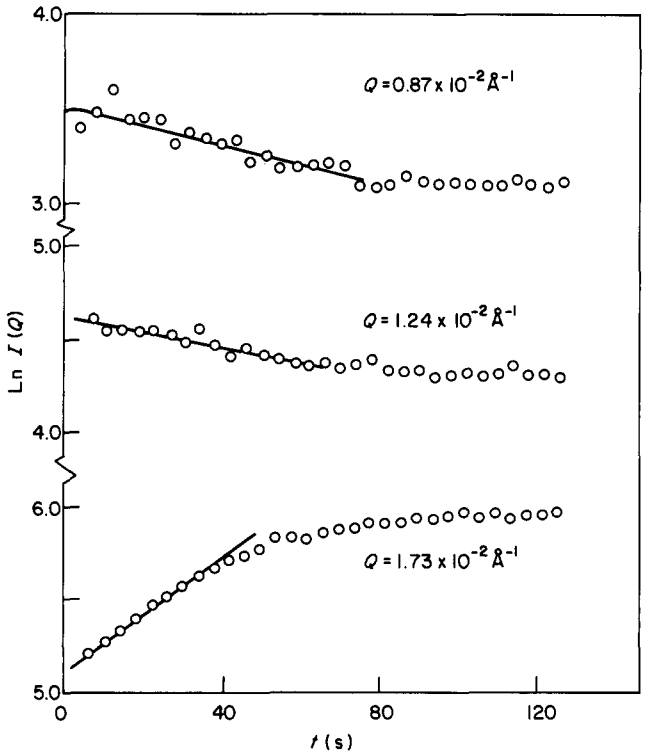

Figure 6 Ln $I(Q)$ plotted as a function of time for selected Q values for S71 quenched from 374 K to 333 K

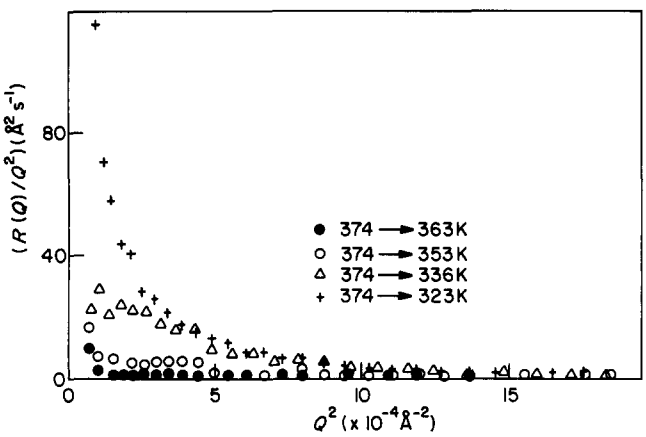

Figure 7 $R(Q)/Q^2$ as a function of Q^2 for S50; quench temperatures as indicated

intensities here decrease with increased time. Notwithstanding this different phenomenology, the dependence of the scattered intensity on time is initially exponential for both circumstances. *Figure 6* shows this for selected Q values; very short-time data (<8 s) have been omitted, since non-exponential behaviour is observed due to the thermal relaxation time of the apparatus as discussed above. Linear least-squares analysis of the linear portions of such curves gave the value of $R(Q)$ in equation (6). An initial analysis of the values of $R(Q)$ can be obtained by plotting $R(Q)/Q^2$ as a function of Q^2. Equation (4) shows that such a plot will reveal information on the product $L_0[-S(Q)^{-1}]$, and if the time-dependent Ginzburg–Landau treatment (TDGL) in combination with RPA theory[21] is correct, then a plot similar to *Figure 1* should be obtained. If the original Cahn–Hilliard theory applies, then equation (13) can be written as:

$$R(Q)/Q^2 = D_e[1 - Q^2/2Q_m^2] \quad (16)$$

whence $D_e = \lim R(Q)/Q^2$.

Figures 7 to *10* show such plots for the four different concentrations investigated here. For the two lower concentrations, S50 and S58, the variation of $R(Q)/Q^2$ is very similar to that observed for homopolymer blends by small-angle light scattering. Conversely, the plots of

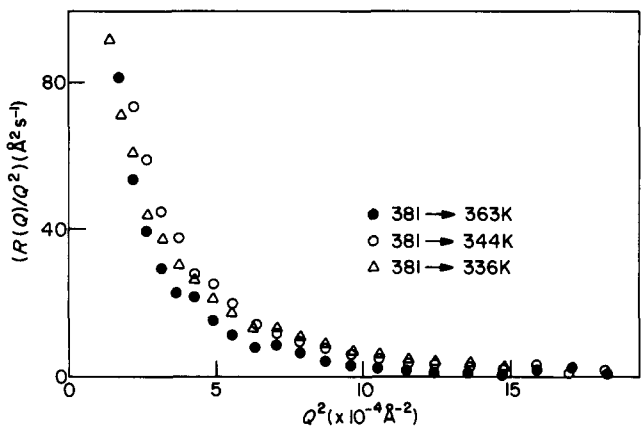

Figure 8 $R(Q)/Q^2$ as a function of Q^2 for S58; quench temperatures as indicated

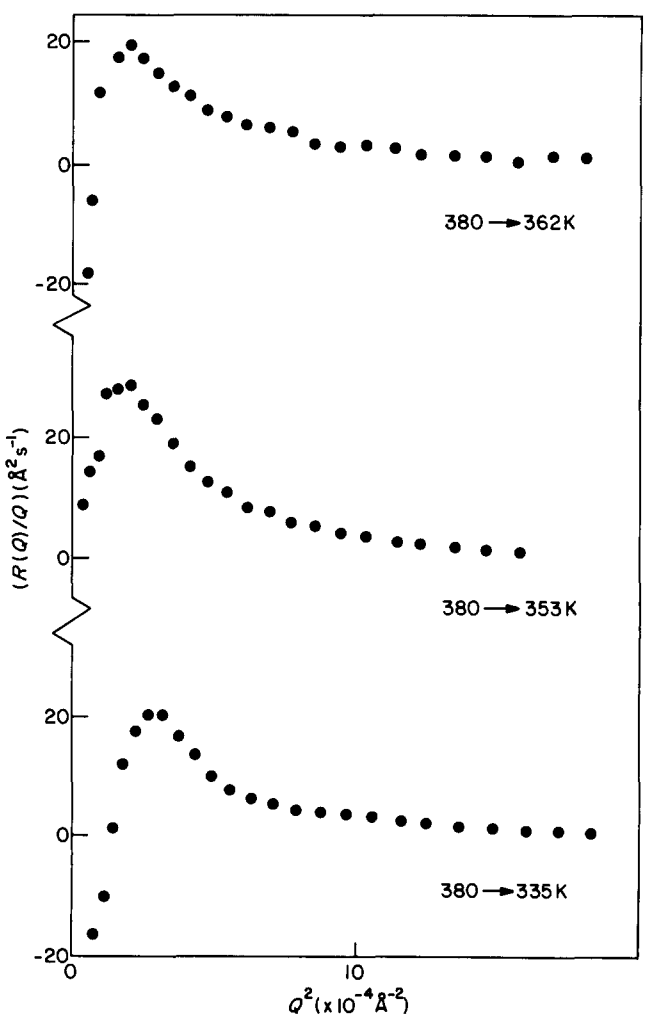

Figure 9 $R(Q)/Q^2$ as a function of Q^2 for S66; quench temperatures as indicated

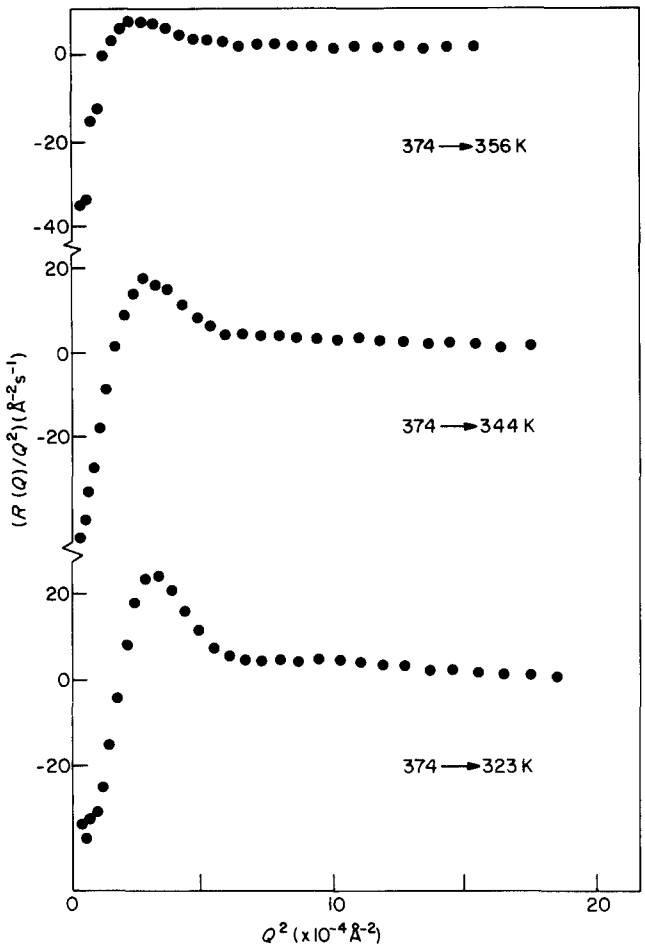

Figure 10 $R(Q)/Q^2$ as a function of Q^2 for S71; quench temperatures as indicated

$R(Q)/Q^2$ for solutions S66 and S71 display the expected maximum at a finite Q value, in qualitative agreement with the theoretical predictions of TDGL theory.

Effective diffusion coefficients

In principle, equation (16) could be used to obtain D_e for solutions S50 and S58 from *Figures 7* and *8*. However, the curvature in these plots and the rapid increase in $R(Q)/Q^2$ at low Q values mean that such values will be subject to large error. Equation (13) has been used to calculate D_e at Q_m, where Q_m is the value at which the maximum scattered intensity was observed in the scattering profile following the quench. The values obtained for all solutions studied are recorded in *Table 3*. Since the interaction parameter χ appears in the expression for $S(Q)$ in $R(Q)$, then D_e will depend on χ. In an earlier paper we evaluated effective values of χ and its temperature dependence for the copolymer solutions studied here. Different values of A and B in equation (17) are obtained for different concentrations of copolymer:

$$\chi = A + B/T \tag{17}$$

Values of D_e at constant χ were interpolated from the values given in *Table 3* by using values of T calculated from equation (17) and use of the appropriate values of A and B valid for each solution. Values of T in equation (17) were chosen such that χ_{eff} in solutions S50, S58, S66 and S71 were identical. Values of T chosen were such that the copolymer systems were all in the homogeneous region. *Figure 11* shows the resulting double logarithmic plot of D_{eff} as a function of polymer concentration. Reptation theory[28] predicts a relation between diffusion coefficient and polymer concentration of:

$$D_{eff} \propto c^{-\alpha} \tag{18}$$

It is evident from *Figure 11* that the exponent in equation (18) does not have a constant value. For the normalized concentration range $0.01 \leqslant C/C_{S66} \leqslant 1$, the slope indicates an exponent of -5, whereas for higher concentrations a much higher value is indicated. The non-observation of a constant value for the exponent in equation (18) is not unusual in studies of diffusive processes in concentrated polymer systems[29,30]. For good solvent systems, reptation theory predicts:

$$D \propto c^{-1.75} \tag{19}$$

while for theta situations, the relation:

$$D \propto c^{-3} \tag{20}$$

is expected.

The 'unusual' values seen here may not be unexpected in view of the rather different situation that prevails for the block copolymer, i.e. in very good solvent conditions for the polyisoprene block but poorer for the polystyrene block.

Table 3 Effective diffusion coefficients calculated from $R(Q_m)/Q_m^2$

Copolymer	Quench temperature (K)	D_{eff} (Å^2 s^{-1})
S50	359.7	3.4 ± 1.6
	353.0	5.3 ± 1.1
	344.0	19.3 ± 0.7
	336.3	16.0 ± 0.5
	323.2	21.5 ± 1.6
S58	363.0	11.4 ± 1.3
	344.4	19.0 ± 0.8
	336.6	26.4 ± 0.8
S66	362.0	12.6 ± 0.8
	353.4	23.5 ± 0.9
	345.0	13.0 ± 0.5
	334.9	20.5 ± 0.5
S71	368.7	0.9 ± 0.6
	363.2	3.0 ± 0.6
	356.4	7.0 ± 0.8
	353.2	12.4 ± 1.3
	350.7	11.5 ± 0.2
	343.8	14.8 ± 0.4
	333.4	20.8 ± 0.8
	323.2	24.1 ± 0.5

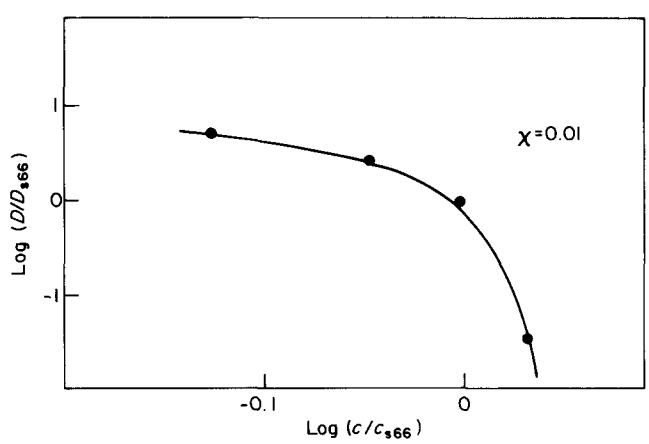

Figure 11 Double logarithmic plot of effective diffusion coefficient at constant χ as a function of concentration

Time-dependent Ginzburg–Landau analysis

Our aims in these experiments were to test the applicability of the Ginzburg–Landau approach suggested by Hashimoto[21]. The use of concentrated solutions leads to a smoothing of the monomer density fluctuations, and hence it is more appropriate to use the original coarse-grained free-energy dependence on Q derived by Leibler[12] using RPA theory. These expressions pertain to the weak segregation limit. Evidently, this type of analysis cannot be used for solutions S50 and S58 and we speculate on the reasons for the observed behaviour of $R(Q)/Q^2$ in these cases below. For solutions S66 and S71, the variation of $R(Q)/Q^2$ with Q^2 is as predicted by the TDGL approach with one difference. In neither solution do we observe an upper critical value of the scattering vector Q above which $R(Q)$ is negative. Instead, $R(Q)$ changes somewhat abruptly to a constant almost zero value. We have neglected random thermal density fluctuations in our approach here and these could contribute to $R(Q)$ at higher Q values leading to the positive values of $R(Q)$ observed. However, we have subtracted the incoherent scattering (that of the solvent mixture) and this has been calculated to be much larger than thermal density fluctuations. Careful examination of *Figure 10* for a deep quench of solution S71 reveals evidence for a second much weaker maximum in $R(Q)/Q^2$ at higher values of Q. It is well known that these systems have a highly ordered microphase-separated state with multiple 'Bragg' peaks. Consequently, we believe that some incipient long-range ordering takes place during the relaxation following a quench and this produces very weak high-Q scattered intensity, which leads to non-negative values of $R(Q)$. Hence, for the evaluation of L_O we have restricted ourselves to data in the region $0 \leqslant Q \leqslant 2.5 \times 10^{-2}$ Å^{-1}. Equation (4) was fitted to the data by a non-linear least-squares method, the value of χ_{eff} in $S(Q)$ pertaining to the initial temperature before the quench. Typical examples of the quality of the fits are shown in *Figure 12*, the values of L_O obtained being listed in *Table 4*. In general, values of L_O increase as the quench depth increases, and since this is related to the mobility, then the interdiffusional mobility increases as the quench depth increases.

To our knowledge there are no published values of L_O in block copolymer systems available; indeed, there are none reported for homopolymer blends since D_{eff} is generally all that is reported. However, Binder[10] has

Table 4 Onsager coefficients from generalized Ginzburg–Landau analysis

Polymer	Initial temperature (K)	Quench temperature (K)	L_O (Å^2 s^{-1})
S66	380.0	362.0	760 ± 3
		353.4	1790 ± 3
		345.0	1280 ± 40
		334.9	3010 ± 7
S71	374.3	368.7	75 ± 1
		363.2	202 ± 14
		356.4	1960 ± 1
		353.2	1390 ± 70
		350.7	2220 ± 90
		343.8	3440 ± 150
		333.4	5300 ± 250
		323.2	6760 ± 260

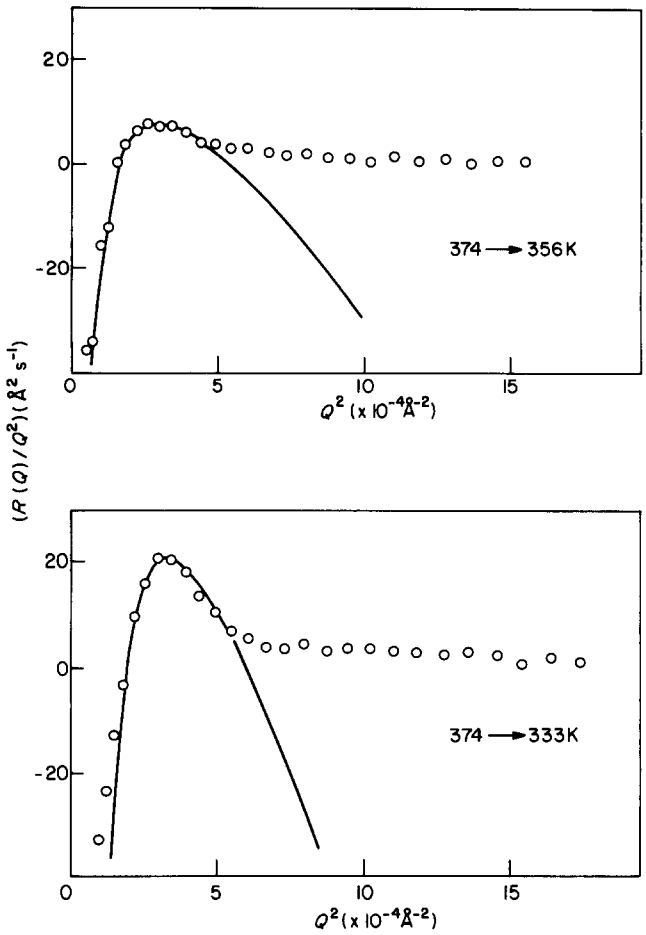

Figure 12 Fit of equation (4) to experimental values of $R(Q)$ for solution S71

provided a relationship for L_O of homopolymer blends:

$$L_O(Q) = (1 - \phi)L_{OA}(Q) \quad (21)$$

$$L_{OA}(Q) = ca^2\phi W_{AA}S_A(Q)/N_A \quad (22)$$

where L_{OA} = the Onsager coefficient for pure polymer A, ϕ = volume fraction of polymer A in the blend, a = statistical step length of polymer A and W_{AA} = mobility of a subunit in polymer A. Note that this factor does not refer to high-frequency intramolecular dynamics but to the (relatively) long-wavelength motions of subunits of the molecule, which are ultimately responsible for reptation. The Q dependence of L_O is explicit in equations (21) and (22) and takes the form suggested by de Gennes[8] and Pincus[9]. In estimating L_O we take the $Q = 0$ limit, where $S_A(Q) = 1$, a is typically 10–20 Å, c is constant of order unity and Binder[10] estimates $10^9 \leqslant W_{AA} \leqslant 10^{11}$ s^{-1}; thus for a degree of polymerization N_A of 100, L_O is then estimated to be $\sim 10^8$–10^{10} Å^2 s^{-1}. Our values in *Table 4* are some 5–7 orders of magnitude smaller than those predicted for homopolymer blends. This may be due to the fact that during interdiffusion accompanying relaxation the blocks in the copolymer molecules are attempting to locate themselves in different regions of space. The connectivity between the blocks prevents this interdiffusion being as rapid as in the homopolymer blend case, and thus L_O is reduced.

Thermodynamic driving force and growth rates

Values of the Onsager coefficient together with experimental values of $R(Q)$ and the radius of gyration R_g,

obtained from the equilibrium scattering at the high initial scattering, can be used to evaluate the Q dependence of the thermodynamic driving force for the growth of the order parameter, i.e. the parameter $R(Q)/L_O Q^2$. Furthermore, the dimensionless factor describing the growth rate, $R(Q)R_g^2/L_O$, of the fluctuations with wavelength of order $Q/2\pi$ are also calculable. *Figures 13* and *14* show each of these parameters calculated from our data for selected temperatures. Surprisingly, the thermodynamic driving force seems to be relatively weak and diffuse when compared to the growth rate obtained using the same value of L_O. This may be due to the use of concentrated solutions making the concentration fluctuations from region to region less sharp even though the value of χ obtained suggests that a strong segregation may prevail. It is also clear that the wavevector of maximum growth rate does not correspond to that where the maximum thermodynamic driving force is observed. The expression for the growth rate is dominated by $R_g^2(\alpha Q_m^{-2})$ and hence this will have its maximum very close to the experimentally observed maximum in the intensity as a function of Q. However, both L_O and $R(Q)$ are obtained from a simplified theory that omits the dependence of free energy on terms in Q of order greater than 2, and it is assumed that L_O is Q-independent.

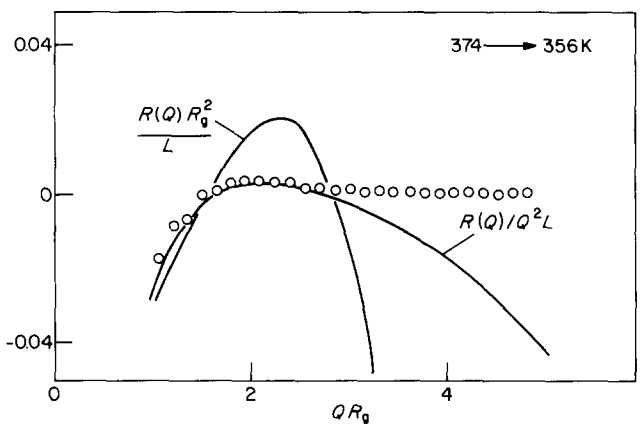

Figure 13 Wavevector dependence of concentration fluctuation growth rate, $R(Q)R_g^2/L_O$, and thermodynamic driving force, $R(Q)/Q^2L_O$, for S66. Quench temperatures indicated. Full curves are calculated from values of $R(Q)$, L_O, R_g; points are experimental values of $R(Q)/Q^2L_O$

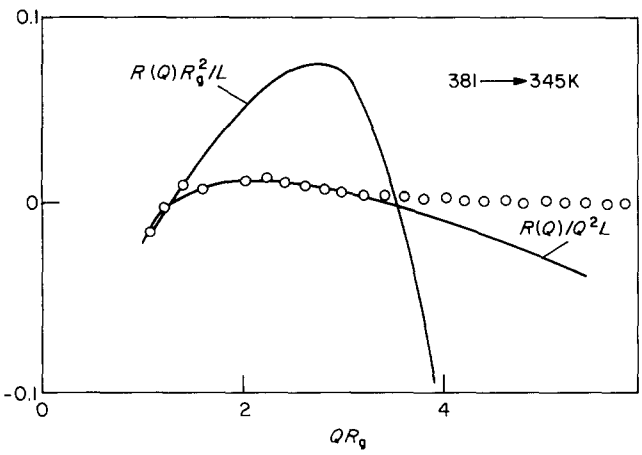

Figure 14 Wavevector dependence of fluctuation growth rate and thermodynamic driving force for copolymer S71 (see *Figure 13*)

Inclusion of such additional factors could well shift the maximum in $R(Q)/L_O Q^2$ to be coincident with the observed maximum growth rate in the SANS profiles.

CONCLUSIONS

We have demonstrated that the observation of the relaxation to a new equilibrium state in a block copolymer following a quench from a high temperature is observable by time-resolved small-angle scattering. The intensity of scattering follows an initially exponential dependence on the time after the quench and this dependence may be negative or positive. Decreases in scattered intensity (negative dependence on time) are observed for high copolymer concentration and low values of the scattering vector Q. For the lower copolymer concentrations ($\leqslant 58\%$), there was no maximum in $R(Q)$, the relaxation rate constant, as a function of Q^2. There could be two sources for this. First, the osmotic swelling of the copolymer could be so large that the maximum in $R(Q)$ is confined to a region of very low Q, which was not accessible in the instrument geometry used here. Secondly, the random-phase approximation is strictly only valid for bulk polymer, and there may well be a lower limit to the concentration below which it is inapplicable since it is no longer a true description of the polymer system.

At higher copolymer concentrations, there is qualitative agreement of the combined time-dependent Ginzburg–Landau theory and the random-phase approximation, in that a maximum in $R(Q)$ is observed and a lower limit to positive values of $R(Q)$ is clearly evident. What is not observed is the upper Q limit to the growth of concentration fluctuations; this we attribute to the incipient long-range ordering becoming evident in the scattered intensity and hence increasing $R(Q)$ values. The values of the Onsager coefficients obtained are in the range $700 \leqslant L_O/\text{A}^2\,\text{s}^{-1} \leqslant 7000$. These values are several orders of magnitude less than predicted values for homopolymer blends. In these latter systems, however, the thermodynamic and hydrodynamic situations are quite different. Lastly, the thermodynamic driving force factor and the growth rate factor calculated from values of L_O, R_g and $R(Q)$ show the expected variation with Q. The maxima are not coincident but for the deeper quenches they tend to approach a common value of Q. Furthermore, for the deeper quenches, there is a slight narrowing of the thermodynamic driving force and growth rate curves, indicating that the fluctuation wavelength equivalent to Q_m is favoured at the expense of others.

All of these conclusions above need to be tempered by the simplifications we have made, i.e. neglect of thermal fluctuations and more importantly the assumption of a Q-independent Onsager coefficient. Nonetheless, it is evident that it is possible to observe the processes leading to microphase separation in block copolymers at a molecular level in real time.

ACKNOWLEDGEMENTS

We thank the Science and Engineering Research Council, UK, for the financial support of this work.

REFERENCES

1 de Gennes, P. G. 'Scaling Concepts in Polymer Physics', Cornell University Press, Ithaca, NY, 1979
2 Sanchez, I. in 'Polymer Blends' (Eds D. R. Paul and S. Newman), Academic Press, New York, 1978, Vol. 1
3 Nishi, T. *CRC Crit. Rev. Solid State, Mater. Sci.* 1986, **12**, 329
4 Strobl, G. in 'Polymer Motion in Dense Systems' (Eds D. Richter and T. Springer), Springer Verlag, Berlin, 1988
5 Izumitani, T. and Hashimoto, T. *J. Chem. Phys.* 1985, **83**, 3694
6 Higgins, J. S., Fruitwala, H. A. and Tomlins, P. E. *Br. Polym. J.* 1989, **21**, 247
7 Cahn, J. W. and Hilliard, J. *J. Chem. Phys.* 1958, **28**, 258
8 de Gennes, P. G. *J. Chem. Phys.* 1980, **72**, 4756
9 Pincus, P. *J. Chem. Phys.* 1981, **75**, 1996
10 Binder, K. *J. Chem. Phys.* 1983, **79**, 6387; *Colloid Polym. Sci.* 1987, **265**, 273
11 Helfand, E. and Wasserman, Z. in 'Developments in Block Copolymers – 1' (Ed. I. Goodman), Elsevier Applied Science, London, 1982, Ch. 4
12 Leibler, L. *Macromolecules* 1980, **13**, 1602
13 Fredrickson, G. and Helfand, E. *J. Chem. Phys.* 1987, **87**, 697
14 Olvera de la Cruz, M. and Sanchez, I. *Macromolecules* 1986, **19**, 2501
15 Mori, K., Tanaka, H. and Hashimoto, T. *Macromolecules* 1987, **20**, 381
16 Mori, K., Hasegawa, H. and Hashimoto, T. *Polym. J.* 1985, **17**, 799
17 Connell, J. G. and Richards, R. W. *Macromolecules* 1990, **23**, 11
18 Hashimoto, T., Ijichi, Y. and Fetters, L. J. *J. Chem. Phys.* 1985, **89**, 2463
19 Fetters, L. J., Richards, R. W. and Thomas, E. L. *Polymer* 1987, **28**, 2252
20 Hashimoto, T., Kowsaka, K., Shibayama, M. and Kawai, H. *Macromolecules* 1986, **19**, 754
21 Hashimoto, T. *Macromolecules* 1987, **20**, 465
22 Gunton, J. D., San Miguel, M. and Sahni, P. S. in 'Phase Transitions and Critical Phenomena' (Eds. C. Domb and J. L. Lebowitz), Academic Press, New York, 1983, Vol. 8, Ch. 3
23 Connell, J. G. and Richards, R. W. *Prog. Colloid Polym. Sci.* 1989, **80**, 180
24 Cook, H. E. *Acta Metall.* 1970, **18**, 297
25 Hashimoto, T. in 'Thermoplastic Elastomers' (Eds N. R. Legge, G. Holden and H. E. Schroeder), Hanser Verlag, Munich, 1987, Ch. 12
26 Connell, J. G. PhD Thesis, University of Strathclyde, 1990
27 Hashimoto, T., Kowsaka, K., Shibayama, M. and Suehiro, S. *Macromolecules* 1986, **19**, 750
28 Doi, M. and Edwards, S. F. 'The Theory of Polymer Dynamics', Oxford University Press, Oxford, 1986
29 Wheeler, L. M. and Lodge, T. P. *Macromolecules* 1989, **22**, 3399
30 Brown, W. and Zhou, P. *Macromolecules* 1989, **22**, 4031